



Reassembling 3D Thin Fragments of Unknown Geometry in Cultural Heritage

ZHENG SHUNYI, HUANG RONGYONG, WANG ZHENG, Wuhan, China & LI JIAN, Zhengzhou, China

Keywords: photogrammetry, reassembling, cultural heritage, matching, adjustment

Summary: Many fragile antiques have already been broken when being discovered at archaeological sites. Such antiques are a precious part of our cultural heritage. However, the fragments cannot be effectively interpreted and studied unless they are successfully reassembled. Additionally, there still exist many problems in the reassembly procedure in existing methods, such as numerical instabilities of curvature and torsion based methods, the limitations of geometric assumptions, the error accumulation of pairwise matching approaches, etc. Regarding these problems, this paper proposes an approach to match the fragments to each other for their original 3D reconstruction. Instead of curvatures and torsions, the approach is based on establishing a local Cartesian coordinate system at every point of the 3D contour curves. First of all, the 3D meshes of the fragments are acquired by a structured-light based method, with the corresponding 3D contour curves extracted from the outer boundaries. The contour curves are matched and aligned to each other by estimating all the possible 3D rigid transformations of the curve pairs based on the local Cartesian coordinate systems, and then the maximum likelihood rigid transformations are selected. Finally, a global refinement is introduced to adjust the alignment errors and improve the final reassembling accuracy. Experiments with several groups of fragments suggest that this approach cannot only match and align fragments effectively, but also improve the accuracy significantly, which promises the potential to be able to apply it to fragments in cultural heritage. Comparing with the original 3D model acquired before being broken, the final reassembling accuracy reaches 0.47 mm.

Zusammenfassung: Zusammenfügen dünner 3D-Fragmente mit unbekannter Geometrie in der Denkmalpflege. Viele antike Fundstücke sind bei ihrer Ausgrabung bereits zerbrochen. Solche Fundstücke sind ein wertvoller Teil unseres Kulturerbes. Die Fragmente können jedoch nicht effektiv interpretiert und studiert werden, solange sie nicht erfolgreich wieder zusammengesetzt worden sind. Bei diesem Zusammenfügen haben aktuelle Verfahren noch viele Probleme, z.B. die numerische Instabilitäten bei auf Krümmung und Torsion basierenden Methoden, die Limitierungen durch Annahmen über die Objektgeometrie oder das kumulative Anwachsen der Fehler bei paarweiser Anpassung der Teile. In diesem Artikel wird eine neue Methode für das Zusammenfügen solcher Fragmente vorgestellt. Statt auf Krümmung und Torsion beruht dieser Ansatz auf der Definition lokaler kartesischer Koordinatensysteme an jedem Punkt der 3D Konturlinien der Fragmente, welche dazu genutzt werden, um die Linien miteinander zu verknüpfen und dadurch das Gesamtobjekt zusammenzustellen. Zunächst werden digitale Oberflächenmodelle durch ein auf strukturiertem Licht basierendes Verfahren erfasst und danach die 3D-Konturlinien aus den Außenkonturen der Modelle extrahiert. Anschließend werden die Konturlinien unter Einbeziehung aller möglichen starren 3D-Transformationen zwischen Punkten auf Kurvenpaaren basierend auf den lokalen kartesischen Koordinaten einander zugeordnet und ausgerichtet. Dabei wird für die Auswahl der am besten passenden Lösungen die Maximum-Likelihood-Methode angewendet. Um die Genauigkeit der Rekombination zu erhöhen, werden im Zuge einer globalen Ausgleichung kumulative Fehler iterativ beseitigt. In mehreren Experimenten mit verschiedenen Gruppen von Fragmenten zeigte sich, dass durch diese Methode nicht nur die dünnen Fragmente der Fundstücke effektiv wieder zusammengesetzt werden konnten, sondern auch die Genauigkeit der wieder zusammengeführten Objekte deutlich gesteigert

werden konnte. Im Vergleich zum ursprünglichen 3D Modell, das vor dem Zerbrechen erstellt worden war, ließ sich eine Genauigkeit der Rekombination

von 0,47 mm erreichen. Das zeigt das vielversprechende Potenzial dieser Methode für die praktische Anwendung in der Denkmalpflege.

1 Introduction

A large quantity of fragile antiques may be found at archaeological sites. Such antiques are a precious part of our cultural heritage, but they are often discovered in broken form due to having been buried for a long time and due to their fragility. They must be reassembled before any other academic procedures. For example, the site's chronology, the population's socioeconomic standards, or even the extent of local or international trade can be indicated by potteries or vessels reconstructed from the found shards. However, most 3D fragments are reassembled and restored manually, so the task requires tedious work from archaeologists and restoration personnel. Thus, a lot of ancient artifacts from fragments found at archaeological sites remain unstudied. Furthermore, the reassembling effects always turn out to depend on the personal experience of the involved archaeologists and restoration personnel, and the excavated fragments are vulnerable in case of any wrong manual operation.

Computer technology can be used to automatically or semi-automatically reassemble such fragments without the risk of damage. However, it is still very challenging to do so because the fragments are thin and do not have surfaces suitable for matching. That is, only the contour curves of the fragments can be utilized for matching and the alignment of adjacent shards. Although there are many methods dealing with such challenges, they have some disadvantages nonetheless. For example, in order to simplify the problem and to improve robustness, some authors (COOPER et al. 2001, WILLIS & COOPER 2004, KAMPPEL et al. 2002, RAZDAN et al. 2001) imposed the assumption of a global model with known geometry to the original object, e.g. assuming the object to be axially symmetric. Such an assumption may not be fulfilled in many cases. Methods relying on representing the curve with shape feature strings, such as curvatures and torsions (KONG & KIMIA 2001, ÜÇOLUK & HAKKI

TOROSLU 1999, GRUEN & AKCA 2005, OXHOLM & NISHINO 2013) are fast. But the main problem is that the computation of curvature and torsion involves up to third-order derivatives, which is sensitive to noise and local discontinuity (WILLIS & COOPER 2008). In addition, the alignment after the matching process necessarily suffers from error accumulation, because it usually relies on a pairwise approach. Even the extension of the pairwise approach (COOPER et al. 2001, KONG & KIMIA 2001), which delays the alignment phase until clusters of three matching fragments have been found, cannot completely improve the alignment accuracy due to local optimization. WILLIS & COOPER (2008) have provided a detailed survey of the state-of-the-art in both automatic and semi-automatic ancient artifact reconstruction systems, including almost all of the current 2D and 3D artifact reconstruction methods and their extensions. However, as is pointed out by WILLIS & COOPER (2008), there are still some aspects to be improved in the future, such as the efficiency, the incorporation of more available information, the development of an information-theoretic basis for searching compatible matches, etc.

PAPAIOANNOU & KARABASSI (2003) combined curve matching techniques with a surface matching algorithm to estimate the positioning and respective matching error for the joining of three-dimensional fragmented objects. FILIPPAS & GEORGOPOULOS (2013) presented the Fragmatch Algorithm that accepted data point clouds as input, i.e. X, Y, and Z for each point of the broken surfaces and not of the whole fragment. HUANG et al. (2006) also presented a system for automatic reassembly of broken 3D solids, in which they developed several new techniques in the area of geometry processing, including the novel integral invariants for computing multi-scale surface characteristics, registration based on forward search techniques and surface consistency, and a non-penetrating iterative closest point algorithm. BROWN et al. (2008) focused on the

specific problem of documenting and reconstructing fragments of wall paintings from the site of Akrotiri on the volcanic island of Thera. They take advantage of the fragments' flat front surfaces to limit their search space to planar transformations.

In general, fragments found at archaeological sites can be divided into two categories: thick and thin fragments. Current research on fragment reassembling can also be divided into aiming at thick and aiming at thin fragments accordingly. This paper focuses on the assembling of 3D thin shards, which cannot be converted into a 2D problem. In other words, an approach is put forward to match and align the shards for recovering their original 3D shapes, which is based on establishing local Cartesian coordinates at every point of the contour curves. The approach is free from any geometry assumption about the original shape and computation of curvatures and torsions. The initial matching and alignment of the proposed approach are both based on a pairwise estimation of the transformations between fragments. Besides, similar to OXHOLM & NISHINO (2013), the alignment is refined global-

ly by utilizing the core functionality of the iterative closest point (ICP) algorithm (BESL & MCKAY 1992). But instead of OXHOLM and NISHINO's original approach that iterates between optimizing the transformations and updating the correspondences of a subset (OXHOLM & NISHINO 2013), this paper takes advantage of the idea of adjustment (TRIGGS et al. 2000) in photogrammetry, which optimizes the transformations of all the fragments in each iteration. In other words, considering the practical necessity of reconstruction of antiques from 3D thin fragments found at archaeological sites, this paper aims to propose an approach to reassemble and reconstruct 3D thin fragments without known geometric shape assumption. The proposed method has the potential to be applied to the restoration of cultural relics from 3D thin fragments with an acceptable accuracy.

In the following sections, this paper will introduce the proposed approach according to the organization as shown in Fig. 1, including data acquisition and pre-processing, initial matching and alignment, global refinement, followed by experiments and an evaluation.

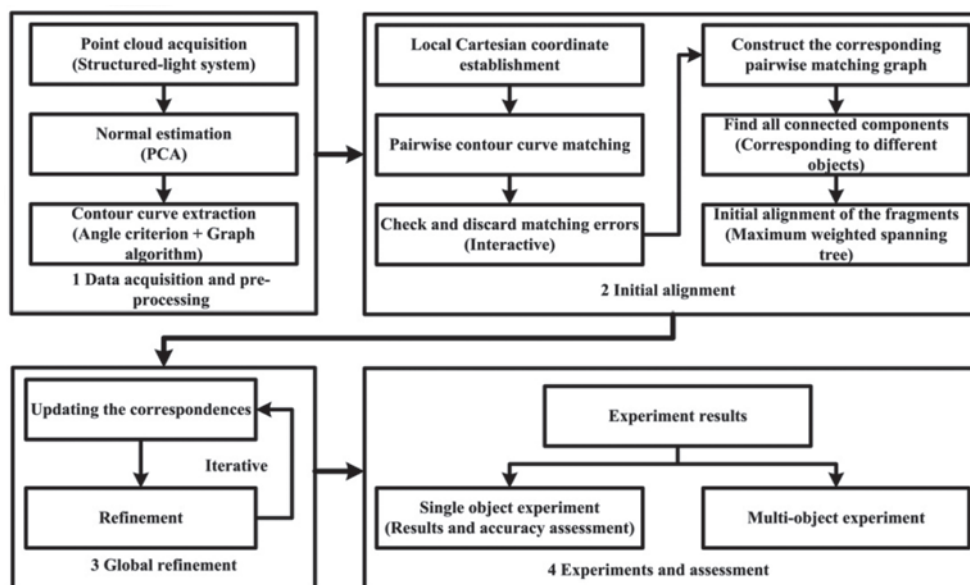


Fig. 1: Paper organizational structure.

2 Data Acquisition and Pre-Processing

Three-dimensional measurement and reconstruction of fragments, which is the prerequisite for reassembling fragments in cultural heritage research, is based on accurate extraction of the fragments' geometry information. In general, any commercially available 3-D laser-scanners are able to digitize fragments. Particularly, with its abilities to acquire reliable, precise, and dense point clouds at a low cost even when objects lack texture, the structured-light based method is chosen in our experiments to extract the fragments' geometry. Many existing structured-light based methods can be used. We utilize the system developed by ZHENG et al. (2012) for that purpose (Fig. 2). After the acquisition of the point cloud, we need to further estimate the surface normals and extract the contour curves for reassembling the fragments.

Like most surface normal estimation schemes (HUANG et al. 2009, RUSU 2010), we also make use of principal component analysis (PCA) (RUSU 2010). As the orientation of the normals computed via PCA is ambiguous, i.e. each normal can direct to two different directions, we need some additional work to compute a consistent normal orientation, and the problem turns out to be very difficult in general. Fortunately, in this paper, we employed a structured-light based system for the data acquisition, so each viewpoint of the point clouds is known as the projective centre of the corresponding camera. As a result, the normals can be consistently oriented towards the known viewpoint. As an example of data ac-

quisition, one broken bowl is shown in Fig. 3, where (a) is the original fragments' photo, and (b) is a visualisation of the corresponding point clouds rendered by their normals.

Note that although our reassembly approach only needs the contours to match the fragments, we need the neighbouring points to estimate the normal of each point of the contours, as described in the next section.

As one of the most important operations of our reassembly approach, contour curves are extracted after the normal estimation is finished. In this paper, an angle criterion that is similar to GUMHOLD et al. (2001) is employed to extract coarse contour curve points. Details are as follows:

- 1) For each point \mathbf{P} in one point cloud, we project \mathbf{P} and its neighbours into a xy-coordinate system orthogonal to the normal direction, where \mathbf{P} is the origin.
- 2) Let β be the maximum angle interval that does not contain any neighbour point in the defined xy-coordinate system. The bigger β is, the higher is the probability that \mathbf{P} is a contour curve point.

If β is larger than a threshold, i.e. 90° in this paper, the corresponding point \mathbf{P} is selected as a candidate contour curve point.

It is obvious that coarse contour curve points are unorganized, and errors are inevitable, as is shown in Fig. 3c. In order to estimate the arc length of contour curves for the following contour curve matching, we need to discard errors and order contour curve points properly as follows:

- 1) Let $G = (V, E)$ be a graph, where V corresponds to the set of all contour candidate points, each edge $e \in E$ connects a



Fig. 2: Structured-light scanning system (ZHENG et al. 2012).

- point $P \in V$ to another point $Q \in V$ in the neighbourhood of P , and the corresponding weight $W(e)$ of e is the length of \overline{PQ} i.e. $W(e) = |\overline{PQ}|$.
- 2) Find the minimum weighted spanning tree $T(G)$ of G , and replace each edge weight of the minimum weighted spanning tree by 1.
 - 3) Find all shortest paths between any pair of vertices in $T(G)$ – we use the Floyd-Warshall algorithm (FLOYD 1962) in our experiments – and then select the path that has the maximum path length as the final extracted contour curve. As a result, the contour curve points can also be ordered along the path.

As can be seen in Fig. 3c, the errors can be successfully excluded in the final ordered contour curves in comparison to the initial ones.

We just make use of these original ordered points instead of the curvatures and torsions to represent the contour curves, thus avoiding the computation of curvatures and torsions.

3 Initial Matching and Alignment

To measure the degree of correspondence between one 3D contour curve and another, a local coordinate system is firstly established at each point of the contour curves (section 3.1). After that, a new similarity measure is used to find pairs of potentially matching fragments (section 3.2). Based on this similarity measure, we apply a pairwise strategy to find the initial matching and alignment of the fragments, i.e. we calculate the similarity measure for every pair of the contour curves of the

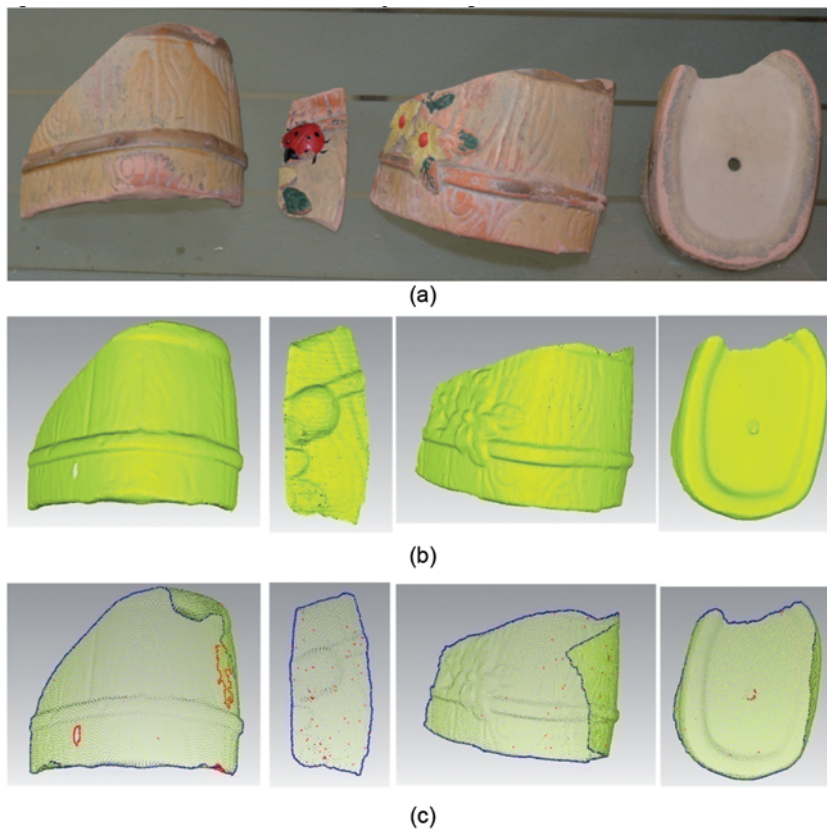


Fig. 3: Geometry information of one broken bowl acquired by a structured-light system: (a) Original fragments of the broken bowl, (b) Point clouds of the fragments rendered by their normals, (c) Coarse and final ordered contour curves, where red points are the discarded errors.

fragments, and then construct a graph to encode the matching degree of all pairs of the contour curves. In the graph, nodes represent individual contour curves of the fragments, and each pair of nodes is connected by an edge weighted by the matching degree of the corresponding two contour curves. As a result, we can find the maximum likelihood matching of the fragments by generating the maximum weighted spanning tree of the graph, and furthermore estimate the initial transformations of the fragments according to the maximum weighted spanning tree.

3.1 Establishment of a Local Coordinate System

When 3D contour curves are extracted successfully, every curve point is associated with a unique normal, which is estimated earlier in the course of normal estimation and contour curve extraction, as is shown in the left of Fig. 4. In order to establish local Cartesian coordinate systems for matching and alignment, the tangent at a curve point is estimated by line fitting based on curve points located in the neighbourhood of that point. After that, the tangential directions of one contour curve are chosen in a way to make sure that the contour curve goes counter-clockwise around the region of the corresponding point cloud, as is shown in the middle of Fig. 4. The local Cartesian coordinate system can be successfully established by the normal and the tangent at the corresponding point: The position of the point is defined as the coordinate origin, the tangent is defined as the x axis, the normal is defined as the z axis, and the y axis is finally

defined by the cross product of z axis and x axis with the right hand rule, as is shown in the right of Fig. 4.

3.2 Pairwise and Multi-piece Matching

Once the local Cartesian coordinate systems are established, the initial pairwise matches of fragments can be found based on the local Cartesian coordinates of the contour curves. When we find a pair of matching points located in two different contour curves, we can estimate the three-dimensional rigid transformation between the two curves according to the local Cartesian coordinates of the matching points. Our pairwise matching algorithm is based on this principle, i.e. we define the similarity measurement from one fragment contour curve to another and design the initial matching and alignment of the fragments as follows:

- 1) For each pair of fragments, we test all combinations of pairs of contours, i.e. for any two contour curve points of the pair, a rigid transformation is estimated according to the corresponding local Cartesian coordinate systems of the point pair, in which the local system of the first fragment is selected as the origin. Then the two contour curves are converted to the same coordinate system by the estimated rigid transformation.
- 2) For any point P_i located in one of the converted curves, we search the nearest point Q_i from the other curve, and then the distance d_i is calculated as follows:

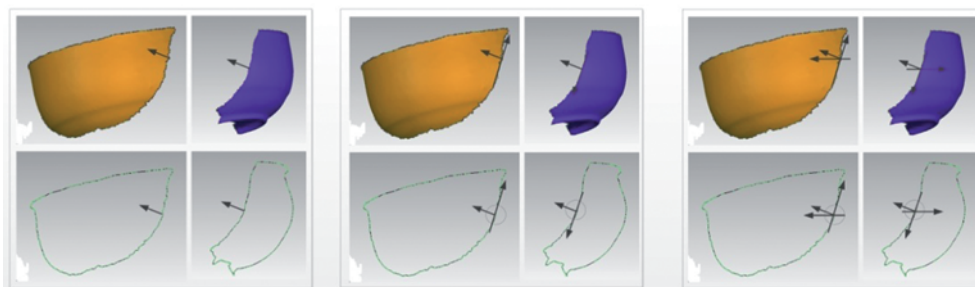


Fig. 4: The establishment of a local Cartesian coordinate system.

$$d_i = \|\mathbf{P}_i - \mathbf{Q}_i\| \quad (1)$$

Finally, we make use of a fixed threshold – about 6 times of the average distance between points on the contour or 2.0 mm in this paper – to distinguish the outliers from the inliers of the matching. The outliers and the inliers are respectively signed **O** and **I** in the follow sections.

- 3) After that, the arc length along the trajectory of the inliers is estimated. The similarity measure proposed in this paper is defined by (2):

$$g_i = \frac{L_i}{c + \sqrt{\frac{\sum_{\mathbf{P}_j \in \mathbf{I}} d_j^2}{N}}} = \frac{L_i}{c + \sqrt{\frac{\sum_{\mathbf{P}_j \in \mathbf{I}} \|\mathbf{P}_j - \mathbf{Q}_j\|^2}{N}}} \quad (2)$$

where c is a constant which is used to avoid the denominator becoming zero under the ideal condition that all residuals are zeroes, and N is the number of the inliers. As the contour curves have been ordered in pre-processing (cf. section 2), the arc length L_i can be easily estimated by adding up all adjacent point pairs' Euclidean distances along the inliers according to the order.

- 4) The matching degree D of this pair of fragments is then computed by finding the maximum g_i value of the contour curve pair:

$$D = \max_i \{g_i\} \quad (3)$$

It should be noted that when we find the maximum g_i value, we can also acquire the max-

imum likelihood alignment of the curve pair because of step (1) above.

In order to align the fragments to a common coordinate system (multi-piece matching), we proceed as follows. As soon as all matching degrees have been calculated, we build a graph in which each vertex represents an individual contour curve, and each pair of the vertices is connected by an edge weighted by the matching degree. We only need $n-1$ pairs of pairwise matchings to align the fragments to a common coordinate system, where n is the number of the fragments of an object. In other words, in order to find the maximum likelihood matching and alignment of the fragments, the maximum weighted spanning tree of the graph is generated, and then the transformations of the fragments to a common coordinate system are estimated based on the spanning tree. An example of the matching and alignment corresponding to the data in Fig. 3 is shown in Fig. 5a and b.

The above process illustrates the basic steps of pairwise matching and alignment, and its feasibility can be seen in Fig. 5. However, there are still some problems needed to solve for more common fragment reassembly, such as the computation of each point pair of the curves is time consuming, and the trouble in reassembling of multi-object fragments. In the following sections, we will further introduce our improvements in solving these problems.

3.3 Sampling Contour Curve Points to Reduce the Computational Complexity

Intuitively, we apply down-sampling of the contour curve points to reduce the computa-

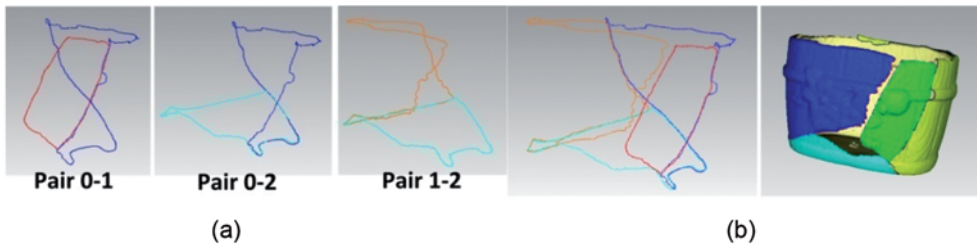


Fig. 5: Pairwise and multi-piece matching examples. (a) Examples for pairwise matching and alignment, (b) Initial multi-piece matching.

tional complexity of the proposed approach. In order to make sure that the down-sampling imposes no significant negative effect on the matching process, we only keep points that have the maximum curvature in a local sense to perform the matching process. However, as is known, almost all curvature and torsion computations suffer from numerical instabilities. Fortunately, we only need a coarse estimation of the curvatures and thus we can calculate the average curvature as proposed by GUMHOLD et al. (2001):

- 1) For each point **P** find two points **A** and **B** so that the arc length $\widehat{AP} = \widehat{PB} = s$ where s is a given constant arc length, i.e. 3.0 mm in the experiments (about 8 times of the average distance between points on the contour).
- 2) Calculate the Euclidean distance between points **A** and **B**, i.e. $d = |\mathbf{AB}|$.
- 3) Calculate the Euclidean distance h from point **P** to line **AB**, as is shown in Fig. 6a.
- 4) Finally, similar to GUMHOLD et al. (2001), the average curvature κ of point **P** can be estimated using the following equation:

$$\kappa = \theta \approx \frac{2s}{R} = \frac{16sh}{d^2 + 4h^2} \quad (4)$$

Once the average curvatures of the contour curve points have been estimated based on (4), the contour curve points can be down-sampled by keeping only points that correspond to local maxima of the average curvature. Consequently, we only need to check the points of the down-sampled sets to find potential matches, with the matching degrees still being calculated based on the original contour curve

points. A typical sampling example can be seen in Fig. 6b, in which 1.199 contour curve points are down-sampled to 72 points.

3.4 Dealing with Wrong Matches of Single- or Multi-Object Fragment Reassembly

In order to deal with wrong matches of single- or multi-object fragment reassembly, we would like to improve our strategy after the pairwise matching process described in section 3.2. To facilitate the further discussion, the weighted graph that encodes the pairwise matching is denoted by $\mathbf{G}' = (\mathbf{V}', \mathbf{E}')$ in the following sections, where \mathbf{V}' is the set of contour curves, the set of edges \mathbf{E}' is based on matching pairs of the contour curves, and according to section 3.2, each edge is weighted by the matching degree defined by (3).

Because it is impossible to know how many objects can be assembled from the given fragments before the reassembling is finished, it is important to identify errors in the pairwise matching and alignments. However, although almost all correct matching pairs have a larger matching degree than the errors, there is a small quantity of erroneous matching pairs also having high matching degrees, as is shown in Fig. 7. It turns out to be very difficult to automatically distinguish the errors from correct matches.

For this reason, it is necessary to introduce some amount of manual work to check the matching results and discard the errors. To reduce the workload, we employ the following strategy:

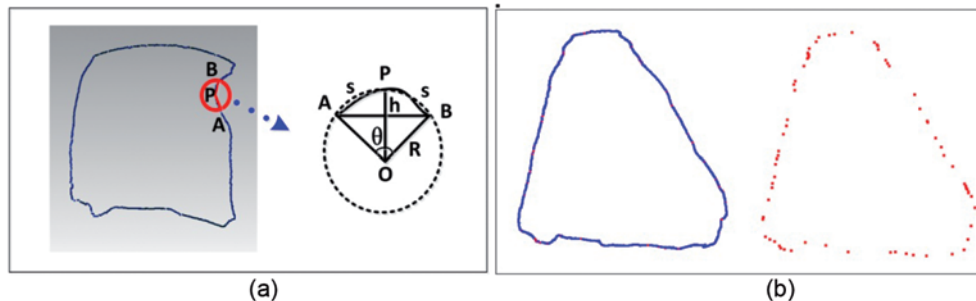


Fig. 6: Down-sampling the contour curve based on local average curvature. (a) Average curvature estimation, (b) Down sampling example.

- 1) For each vertex of G' , we order the corresponding incidence edges according to their weights.
- 2) We check whether the edges correspond to correct matches interactively: For each vertex, only a certain percentage of the incidence edges with the largest weights have to be checked. That is, if a certain percentage of the incidence edges prove to be correct matching pairs, then the checking work of this vertex can stop, and the user can go on to check other vertices. Besides, all the edges that found to correspond to correct matching pairs are labelled as "correct" in this step.
- 3) When all the vertices are checked, we discard all the edges that are not labelled to be correct, so a new graph $G'' = (V', E'')$ can be induced from the graph G' . This graph G'' has the same vertices as the graph G' , and E'' is the edge subset consisting only of the correct matching pairs.

According to the construction of graph G'' , each connected component of G'' corresponds to a possible reassembly object, so we can extract all the connected components to find the number of the reassembly objects. For each connected component, we can easily find the maximum likelihood matching and alignment through its maximum weighted spanning tree, which is similar to the process described in section 3.2.

4 Global Refinement

Due to the employment of pairwise matching strategy, the matching and alignment suffers from serious error accumulation, as is shown in Fig. 9a. For the sake of a higher accuracy,

the alignment errors are iteratively and globally adjusted by a least-square method.

Suppose R_i and T_i are the rotation matrix and the translation vector, respectively, of the rigid transformation to the common coordinate system of the i -th fragment, which have been estimated by the initial matching and alignment proposed in section 3, i.e.

$$P_g = R_i P_i + T_i \quad (5)$$

$$n_g = R_i n_i \quad (6)$$

where P_i is one point in the i -th fragment, P_g is the corresponding point in the common coordinate system, and n_i and n_g are the corresponding normal vectors.

In order to adjust the alignment errors effectively, we need to search for the nearest points of a given point from other contour curves according to the current alignment. Suppose that $P_i^{(j)}$ is one point in the i -th contour curve of the fragments, we can convert it to the coordinate system of the j -th contour curve using the following equation:

$$P_i^{(j)} = R_j^T [R_i P_i^{(j)} + T_i - T_j] \quad (7)$$

The nearest point to $P_i^{(j)}$ is easy to be found in the j -th contour curve according to the coordinate system of the j -th fragment. Then our least-square method is equivalent to searching the minimum of the following function:

$$\begin{aligned} & C \left(\bigcup_i \{R_i \quad T_i\} \right) \\ &= w \sum_{i \neq j} \|P_g^{(i)} - P_g^{(j)}\|^2 + (1-w) \sum_{i \neq j} \|n_g^{(i)} - n_g^{(j)}\|^2 \\ &= w \sum_{i \neq j} \|R_i P_i^{(i)} - R_j P_j^{(j)} + T_i - T_j\|^2 \\ &\quad + (1-w) \sum_{i \neq j} \|R_i n_i^{(i)} - R_j n_j^{(j)}\|^2 \end{aligned} \quad (8)$$

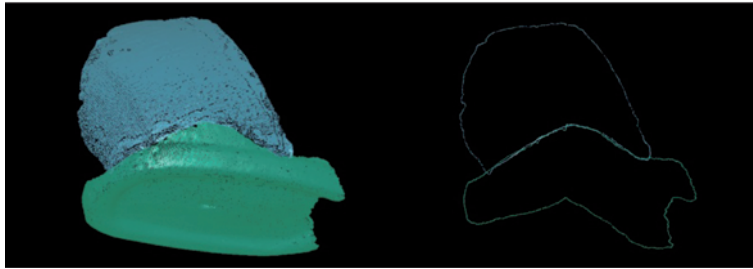


Fig. 7: Example of a false matched pair that has produced a large matching degree.

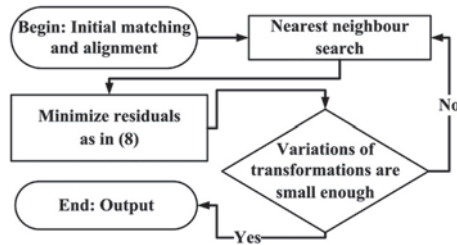


Fig. 8: Diagram of global refinement. Nearest Neighbour Search: For every point $\mathbf{P}^{(i)}$ in one of the contour curves, its nearest point is searched from other contour curves. If the distance to each other are larger than a given threshold (about 6 times of the average distance or 2.0 mm in this paper), the nearest point pair is discarded as a gross error.

where w is the weight for the first term of the function, which is between 0 and 1, $\mathbf{P}_i^{(i)}$ and $\mathbf{P}_j^{(j)}$ are the nearest pairs of points in the i -th and the j -th fragment respectively, $\mathbf{P}_g^{(i)}$ and $\mathbf{P}_g^{(j)}$ are the point coordinates corresponding to $\mathbf{P}_i^{(i)}$ and $\mathbf{P}_j^{(j)}$ in the estimated common coordinate system, and $\mathbf{n}_i^{(i)}$, $\mathbf{n}_j^{(j)}$, $\mathbf{n}_g^{(i)}$, and $\mathbf{n}_g^{(j)}$ are the corresponding normals.

The global refinement by adjusting the alignment errors is summarized in the diagram in Fig. 8.

The global refinement reduces the matching and alignment errors, as is shown in Fig. 9. Note that we can also employ the above global refinement process to deal with the multi-object fragment reassembling problem, because the multi-object fragments can be divided into several connected components according to section 3.4, and the components can be processed individually.

5 Experiments and Evaluation

5.1 Single Object Experiments

The proposed method has been tested on two additional groups of thin fragments to verify the effectiveness of the proposed reassembly approach. As is shown in Fig. 10, our experimental data contains three groups of fragments, namely Data I (5 pieces), Data II (4 pieces), and Data III (12 pieces); note that the broken bowl in Data II was used to illustrate our methodology in the previous sections. The experimental results of reassembling of Data II have already been illustrated in Fig. 9. The results of Data I and Data III are shown in Figs. 11 and 12 respectively. These results indicate that the proposed approach appears to be applicable and that the results are significantly improved due to the introduction of our global refinement. What is more, as original three-dimensional geometry models of our experimental data have been constructed before the corresponding objects were broken, we can assess the reconstruction results quantitatively in section 5.3, which will further support the mentioned conclusion.

5.2 Multi-Object Experiments

As described in section 3.4, we need to introduce some amount of manual work to check the matching results and discard the errors interactively. This strategy divides the multi-object reassembling problem into several sub-problems after the pairwise matching, so that the proposed global refinement process can be applied to tackle the sub-problems, as is shown in Fig. 13. In the experiment, we mixed

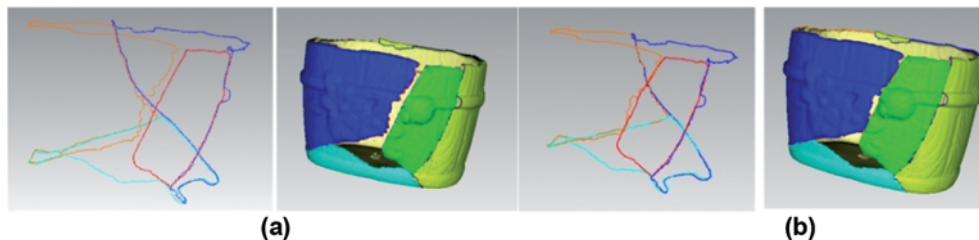


Fig. 9: Global refinement result: (a) Initial multi-piece matching, (b) Global refinement.

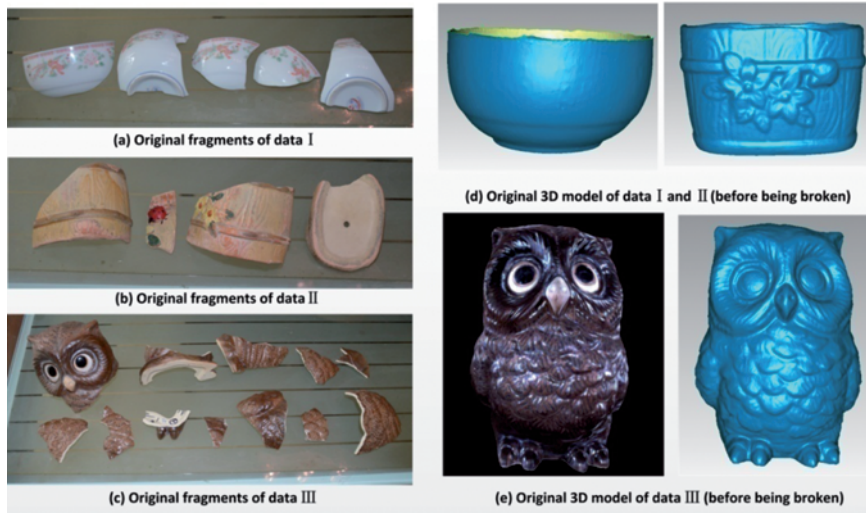


Fig. 10: Experimental data.

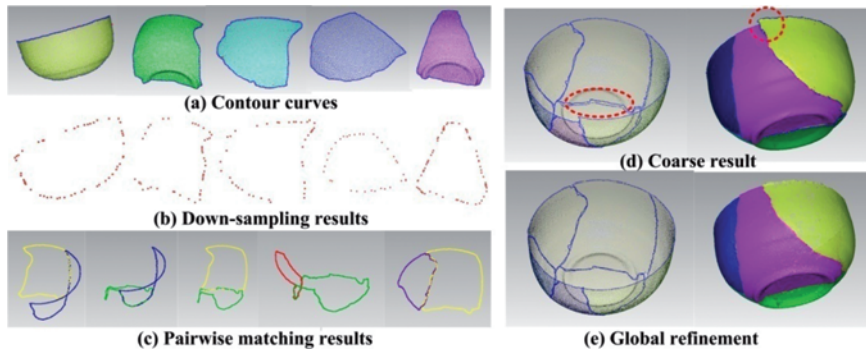


Fig. 11: Reassembling result of data I.

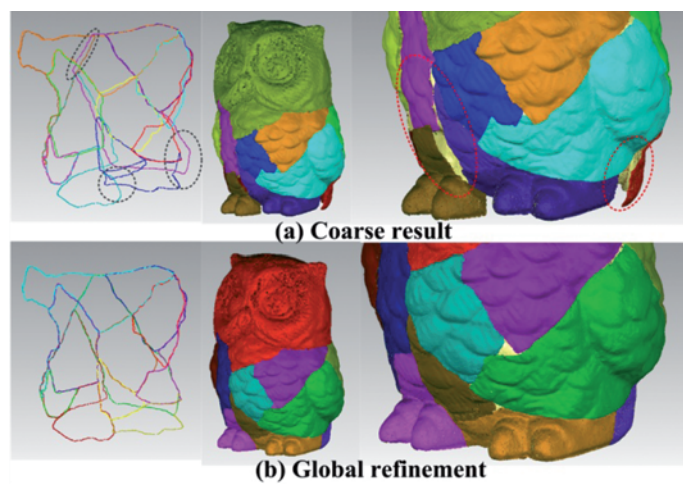


Fig. 12: Reassembling result of data III.

the three fragment sets, and then employed the proposed multi-object strategy to extract different objects through finding all the connected components of the induced sub-graph of the pairwise matching graph. Fig. 13 shows that the three different objects are successfully reassembled and the final global refinement promises the same effects as the single object

experiments for every component (less than 105 pairs are manually checked in Fig. 13).

5.3 Evaluation

In order to assess the external accuracy of the proposed approach, we firstly make use of the

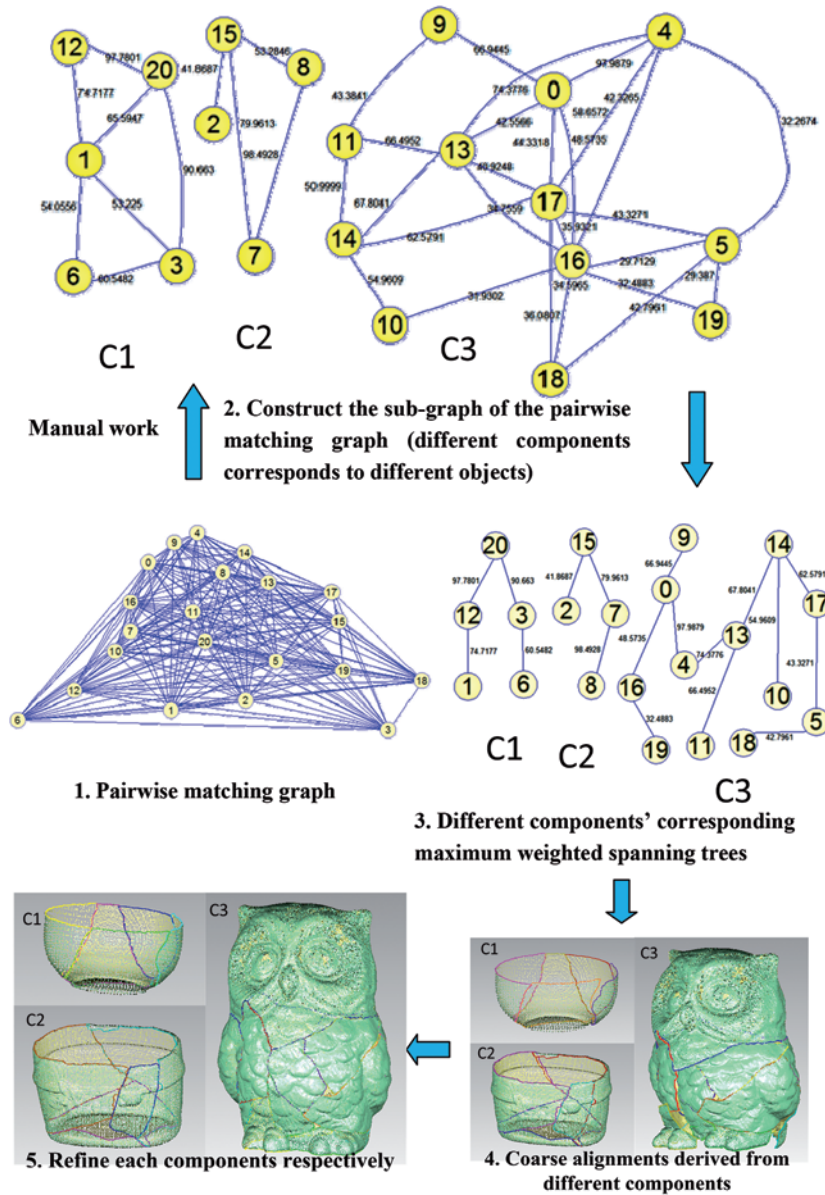


Fig. 13: Multi-object reassembling procedure and result.

Tab. 1: Statistics of reassembling errors before and after global refinement (mm).

Item	Coarse result				Global refinement			
	RMSE	Mean	Min	Max	RMSE	Mean	Min	Max
Data I	0.64	-0.173	-4.28	1.92	0.13	-0.001	-1.52	1.13
Data II	0.65	0.129	-1.84	4.39	0.16	-0.014	-1.74	1.88
Data III	1.12	-0.244	-12.05	7.86	0.47	-0.040	-1.99	1.66

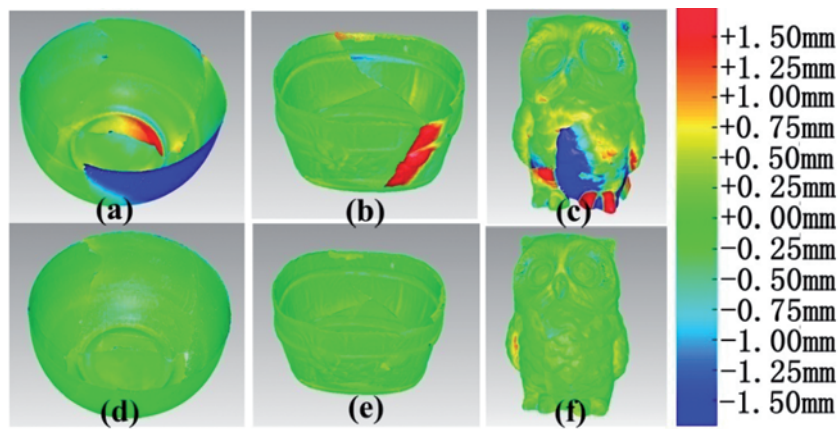


Fig. 14: Alignment errors, where (a), (b), and (c) illustrate the error distributions with respect to Data I, Data II, and Data III before the global refinement, and then (d), (e), and (f) illustrate the corresponding error distributions after the global refinement.

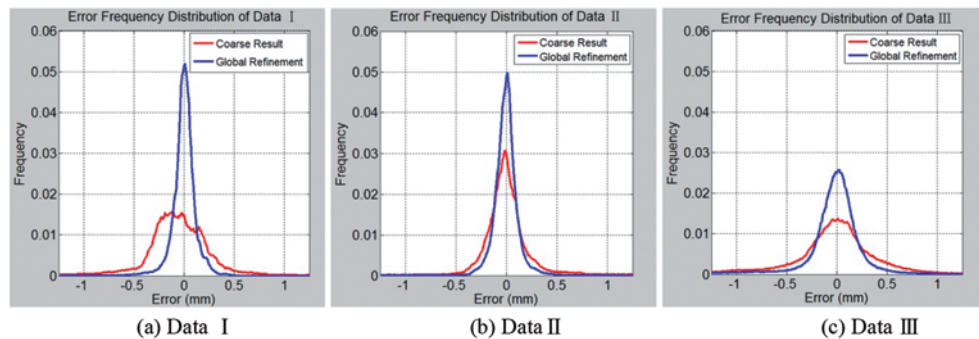


Fig. 15: Error distribution of results.

ICP algorithm (BESL & MCKAY 1992) to align the 3D model reassembled by the proposed approach with the original 3D model acquired before being broken. After that, errors are determined by estimating the directed distances from each point in the reassembled model to the original model's surface. Specifically, for each point in the reassembled model, we search the nearest point in the original model. Then the local tangent plane of the nearest point is obtained, taking into consideration the corresponding normal. Finally, the corresponding error is estimated by the directed distance from the point of the original reassembled model to the local tangent plane.

To exhibit the error distributions of different data before and after the global refinement, we render the errors of the reassembled models with false colours, as shown in Fig. 14. Furthermore, errors of Data I, Data II, and Data III are illustrated by their distribution in Fig. 15, where we can find that when the spatial information is ignored, errors of the test data are consistent with normal distributions before and after the global refinement. Accordingly, statistics of the reassembling errors are calculated and shown in Tab. 1 in detail. Tab. 1 shows that the root-mean-square error (RMSE) of Data I, Data II, and Data III can reach 0.13 mm, 0.16 mm, and 0.47 mm respectively. The RMSE here is calculated by the following equation:

$$RMSE = \sqrt{\frac{1}{N} \sum_i e_i^2} \quad (9)$$

where e_i is the i -th point error of the reassembled model, and N is the number of errors.

In summary, the proposed method is able to successfully reassemble the fragments of all test datasets. Moreover, the accuracies are significantly improved due to the introduction of the global refinement. Original models have also been constructed by the same structured-light scanning system, thus they have the same accuracy as each of the fragments. As the data is acquired at a distance of about 60 cm, the accuracy of the data is about 0.07 mm (about 0.10 mm while comparing two models) according to the reports of ZHENG et al. (2012). However, RMSEs of Data I, Data II, and Data III are 0.13 mm, 0.16 mm, and 0.47 mm respectively after the global refinement, which are larger than the structured-light scanning system's accuracy, but much less than the accuracies before the global refinement. There are four main reasons why RMSEs are larger than the structured-light scanning system's accuracy:

- 1) The presence of some damages in each fragments, e.g. losing of some small shards, losing of parts of the contour curves, and parts of the edges being round, etc.
- 2) The contour curves cannot supply as much information as usual surface-based ICP to reassemble and align the fragments. However, contour curves are generally the only constraints that can be used to reassemble the fragments.
- 3) The average sampling distance of each of our experimental data ranges from 0.30 mm to 0.45 mm, and the extracted contour curve points cannot always locate in the true edges of the fragments, thus the accuracy of the contour curves is expected

Tab. 2: Computation times for different stages of our algorithm.

	MO	TO (s/pair)	MS	TS (s/pair)	TG (s)
Data I	1249	--	70	22.3	4.2
Data II	806	2655.2	48	8.1	5.5
Data III	1638	--	89	54.5	29.6
Mixed Data	1366	--	75	42.2	39.3

MO = Mean number of curvature points, TO = Mean processing time of pairwise matching, MS = Mean number of sampled curvature points, TS = Mean processing time of pairwise matching based on sampled contour points, TG = Mean processing time of global refinement, Mixed Data = Multi-object experiments' data, and "--" indicates that the time is more than 3600.0 s (one hour).

to be lower than the structured-light scanning system's accuracy, i.e. the measurement accuracy.

- 4) Errors are also related to the number of fragments of the reassembled object. As is illustrated in the figures and the table, the errors of Data III are larger than both of Data I and Data II, mainly due to a greater number fragments contained in Data III. Even so, global refinement provides the proposed approach with the potential to be applied to reassemble thin 3D fragments from archaeological sites with an acceptable accuracy.

In our experiments, the reassembling program was developed with C++ and executed with an Asus notebook (Intel (R) Core (TM) i5-2450M CPU @ 2.50GHz (4 CPUs), ~2.50GHz, 4096 MB RAM, Windows 7) in a single thread, and the time consumption is summarized and shown in Tab. 2.

As shown Tab. 2, most of the time is spent in pairwise matching. Pairwise matching is so time consuming that it is impossible to reassemble the fragments when the original contour curves are used in the matching directly. Meanwhile, the sampling process makes the time consumption acceptable in the experiments.

6 Conclusions and Future Work

We have proposed an approach that has the potential to reassemble broken thin 3D fragments found at archaeological sites with an acceptable accuracy. In order to avoid the computation of the curvatures and torsions for matching the fragments' 3D contour curves, this approach defines and calculates a local 3D Cartesian coordinate at every contour curve point, and develops a method to find the maximum likelihood matching pairs of the contour curves. Unlike other current methods, this work does not rely on any assumption about the geometry of the original objects. Together with the maximum likelihood matching, the initial multi-piece alignment of the fragments is also accomplished simultaneously. However, the initial alignment suffers from serious error accumulation. In order to avoid this, we introduce a global refinement meth-

od to adjust the errors and improve the reassembling accuracy. Finally, experiments with several groups of fragments suggest that the proposed approach is able to align fragments successfully. Comparing the reassembled 3D model with the original one, the accuracy of the final model reaches acceptable dimensions (maximum of 0.47 mm) by integrating global refinement. This promises the potential of the proposed method to reassemble thin 3D fragments in archaeological sites. Besides, several schemes are also proposed in this paper to reduce the computational complexity and adapt our method to multi-object cases, and they are also shown to be feasible in the experiments.

However, further research is still needed in order to apply our method to more realistic reassembling projects. For example, because the computation will increase with an increasing number of fragments, we need to further improve the pairwise initial matching and alignment strategy, e.g. using efficient matching methods based on RANSAC (FISCHLER & BOLLES 1981). Furthermore, it is necessary to incorporate other information, e.g. texture, colour, and meeting point of 3 contours, etc., to adapt to the case of multi-object fragments for more automation. In a nutshell, this method still needs improvement for more complex real conditions in the future.

Acknowledgement

This research is supported by the Chinese National Natural Science Foundation Program (No. 41171357, No. 41301518). We are very grateful to the ISPRS Technical Commission V Symposium for the comments and suggestions for our researches, and special thanks are also given to the anonymous reviewers and members of the editorial board for their suggestions of improving this article.

References

- BESL, P.J. & MCKAY, N.D., 1992: A Method for Registration of 3-D Shapes. – *IEEE Transactions on Pattern Analysis and Machine Intelligence* **14** (2): 239–256.
- BROWN, B.J., TOLER-FRANKLIN, C., NEHAB, D., BURNS, M., DOBKIN, D., VLACHOPOULOS, A., DOU-

- MAS, C., RUSINKIEWICZ, S. & WEYRICH, T., 2008: A System for High-Volume Acquisition and Matching of Fresco Fragments: Reassembling Theran Wall Paintings. – *ACM Transactions on Graphics* **27** (3): Article 84: 1–9.
- COOPER, D.B., WILLIS, A., ANDREWS, S., BAKER, J., CAO, Y., HAN, D., KANG, K., KONG, W., LEYMARIE, F.F. & ORRIOLS, X., 2001: Assembling Virtual Pots from 3D Measurements of Their Fragments. – *VAST 2001 Virtual Reality, Archaeology, and Cultural Heritage*, ACM: 241–254, New York, NY, USA.
- FILIPPAS, D. & GEORGOPOULOS, A., 2013: Development of an Algorithmic Procedure for the Detection of Conjugate Fragments. – *ISPRS Annals – Volume II-5/W1, 2013 TC V XXIV International CIPA Symposium* **2–6**: 127–132, Strasbourg, France.
- FISCHLER, M.A. & BOLLES, R.C., 1981: Random sample consensus: a paradigm for model fitting with applications to image analysis and automated cartography. – *Communications of the Association for Computing Machinery* **6**: 381–395.
- FLOYD, R.W., 1962: Algorithm 97: shortest path. – *Communications of the ACM* **5** (6): 345.
- GRUEN, A. & AKCA, D., 2005: Least Squares 3D Surface and Curve Matching. – *ISPRS Journal of Photogrammetry and Remote Sensing* **59** (3): 151–174.
- GUMHOLD, S., WANG, X. & MACLEON, R., 2001: Feature Extraction from Point Clouds. – 10th International Meshing Roundtable: 293–305.
- HUANG, H., LI, D., ZHANG, H., ASCHER, U. & COHENOR, D., 2009: Consolidation of Unorganized Point Clouds for Surface Reconstruction. – *ACM Transactions on Graphics (TOG)* **28** (5): 176.
- HUANG, Q., FLÖRY, S., GELFAND, N., HOFER, M. & POTTMANN, H., 2006: Reassembling Fractured Objects by Geometric Matching. – *ACM Transactions on Graphics (TOG)*: 569–578, New York, NY, USA.
- KAMPEL, M., SABLATNIG, R. & MARA, H., 2002: Automated Documentation System of Pottery. – 1st International Workshop On 3D Virtual Heritage: 14–20, Geneva, Switzerland.
- KONG, W. & KIMIA, B.B., 2001: On Solving 2D and 3D Puzzles Using Curve Matching. – *Computer Vision and Pattern Recognition (CVPR) 2001*, IEEE Computer Society Conference **2** (II): 583–590.
- OXHOLM, G. & NISHINO, K., 2013: A Flexible Approach to Reassembling Thin Artifacts of Unknown Geometry. – *Journal of Cultural Heritage* **14** (1): 51–61.
- PAPAIANOANNOU, G. & KARABASSI, E., 2003: On the Automatic Assemblage of Arbitrary Broken Solid Artifacts. – *Image and Vision Computing* **21** (5): 401–412.
- RAZDAN, A., LIU, D., BAE, M., ZHU, M., FARIN, G., SIMON, A. & HENDERSON, M., 2001: Using geometric modeling for archiving and searching 3d archaeological vessels. – *CISST: 25–28*, Las Vegas, NV, USA.
- RUSU, R.B., 2010: Semantic 3D Object Maps for Everyday Manipulation in Human Living Environments. – *KI-Künstliche Intelligenz* **24** (4): 345–348.
- TRIGGS, B., McLAUCHLAN, P.F., HARTLEY, R.I. & FITZGIBBON, A.W., 2000: Bundle Adjustment – a Modern Synthesis Vision Algorithms. – *Theory and Practice*: 298–372, Springer.
- ÜÇOLUK, G. & HAKKI TOROSLU, I., 1999: Automatic Reconstruction of Broken 3D Surface Objects. – *Computers & Graphics* **23** (4): 573–582.
- WILLIS, A.R. & COOPER, D.B., 2004: Bayesian Assembly of 3D Axially Symmetric Shapes from Fragments. – *Computer Vision and Pattern Recognition*, IEEE Computer Society Conference **1** (I): 82–89.
- WILLIS, A.R. & COOPER, D.B., 2008: Computational reconstruction of ancient artifacts. – *Signal Processing Magazine*, IEEE **25** (4): 65–83.
- ZHENG, S.Y., ZHOU, Y., HUANG, R.Y., ZHOU, L.M., XU, X. & WANG, C.Y., 2012: A Method of 3D Measurement and Reconstruction for Cultural Relics in Museums. – XXII International Society for Photogrammetry & Remote Sensing Congress, Melbourne, Australia.

Addresses of the Authors:

Prof. Dr.-Ing. ZHENG SHUNYI, PD Dr.-Ing. HUANG RONGYONG & M.Sc. WANG ZHENG, School of Remote Sensing and Information Engineering, Wuhan University, No. 129 Luoyu Road, Wuhan 430079, PR China, Tel.: +86-027-68778010, Fax: +86-027-68778010, e-mail: syzheng@263.net, {hry} {zheng.wang}@whu.edu.cn

PD Dr.-Ing. LI JIAN, College of Water Conservancy & Environment Engineering, Zhengzhou University, No.100 Science Avenue, Zhengzhou 450001, PR China, Tel.: +86-0371-68771852, Fax: +86-0371-68771852, e-mail: lijian5277@163.com

Manuskript eingereicht: September 2014
Angenommen: März 2015